

## **Indigenous facility development for studying an elementary radiation process: atomic-field bremsstrahlung**

R. Shanker and S. K. Goel

Atomic Physics Laboratory, Physics Department  
Banaras Hindu University, Varanasi - 221 005, INDIA

**Abstract:** An indigenous setup for studying the process of atomic-field bremsstrahlung produced from the interaction of keV electrons with a solid or a gaseous target has been developed and described. The setup consists of a high-vacuum scattering chamber, a home-built keV electron gun with a replaceable tungsten filament cathode, an isolated floating high-voltage control unit, signal processing electronic modules and a data-acquisition system comprising of an IBM PC/XT 4-K multichannel analyser. The performance of the setup has been tested and used for accumulating data for bremsstrahlung spectra from 7.0 keV electrons incident on thin Ag and Au targets. These spectra have been analyzed and discussed in light of the semiclassical and the quantum calculations. The agreement between experiment and theory is found to be satisfactory within the experimental uncertainty of the measurements.

**Keywords:** atomic-field bremsstrahlung, electron gun, isolated floating high-voltage system, doubly-differential cross section

**PACS numbers:** 29.25.Bx, 32.30.Rj, 34.80.-i

### **1. Introduction**

Atomic-field bremsstrahlung (AFB) has been known for sometime with the realization that when a monoenergetic electron scatters elastically from

an atom/ion/molecule, a photon of a continuous energy is emitted. This radiation forms a continuous x-ray background ranging in energy from the incident energy of the electron down to zero. The intensity of such a radiation is known to depend on the atomic number ( $Z$ ) of the atom being bombarded, the photon energy ( $k$ ), emitted and on the energy of incident electron ( $T$ ). The current theoretical understanding of the AFB has been reviewed by Pratt [1] while experimental procedures and data collections with a thin solid and a gaseous target has been given by Nakel [2], Quarles and his coworkers [3] and by Hippler et al [4].

The major motivation of the present work has based on the following points:

- (i) No experimental facility of the kind described here is operative in any place around the country.
- (ii) There is a great need of experimental data for electron bremsstrahlung at keV energies for testing the existing theories (both thick- and thin-target formulations).
- (iii) It is realized that there is a demand and concern for developing the indigenous components of the experimental setup in the laboratory itself and for creating a culture of designing and fabricating the equipments for use in research and training areas. As a matter of fact, the above objectives have invited a challenging task for any researcher in the country or elsewhere. The efforts made in the present work are directed to achieve the said goals within the constraints of available infrastructural facilities and research funds.

## 2. Why to study AFB at keV energies?

The study of atomic field bremsstrahlung at keV energies is desirable due to the following reasons:

- (i) Most experiments on AFB have been carried out at higher energies (above 50 keV), where the cross sections are larger but less sensitive to atomic structures.
- (ii) The bremsstrahlung process exhibits many of the regimes of physics as we trace the transition from classical to quantum physics; the transition from non-relativistic to relativistic physics.
- (iii) The bremsstrahlung process is expected to help in interpreting and modeling the laboratory fusion and astrophysical problems; also in providing information on designing and controlling the biological exposures to radiation.
- (iv) The bremsstrahlung process becomes important energy-loss mecha-

nism particularly, in fusion plasmas.

- (v) Low-energy electron bremsstrahlung provides an effective tool to determine the number and energy of superthermal electrons generated by the laser-plasma interactions.
- (vi) Study of the bremsstrahlung process helps in basic understanding of the elementary radiation process itself.

Keeping the above objectives in view, we in Atomic Physics Laboratory, Department of Physics, have developed such an experimental setup in recent years. The facility was designed, fabricated, tested, optimized and was finally used to accumulate data on a chosen problem. A more detailed description of the setup has been reported elsewhere [5]. In this talk, I shall, however, present, briefly, various components used in the setup with regard to their designing and optimizing parameters and discuss some bremsstrahlung spectra with thin solid targets in light of available theoretical formulations.

### **3. Development of the AFB experimental setup**

The major components of the AFB setup are the following:

- (i) a high-vacuum scattering chamber;
- (ii) a high-voltage electron gun with a replaceable filament;
- (iii) an isolated floating high-voltage control unit;
- (iv) a high-vacuum pumping system;
- (v) a signal processing and a data acquisition system.

In our setup, the high-vacuum scattering chamber comprises a main scattering chamber, a Faraday cup, a target device and a rotatable arrangement for an x-ray photon detector. The design and fabrication of each of the above components are briefly described in the following subsections. A schematic diagram of the complete AFB setup is shown in Fig. 1.

#### **3.1 High-vacuum scattering chamber**

The main scattering chamber is a cylindrical stainless steel (SS) pipe of 190 mm height and 44 mm inner diameter. The two collinear ports each fitted with a KF10 coupling are used to adopt an electron-gun enclosure on one side and a Faraday cup on the other. Two slots of 8.0 mm height are cut in the SS pipe on both sides of the collinear ports in a horizontal plane containing the electron-beam, the centre of the target and the axis of the Si(Li) photon detector. Slots are covered with a 6  $\mu\text{m}$  thick hostaphan foil which is strong enough to withstand the pressure inside the main chamber and is transparent enough to transmit most of the x-rays. The top flange of the scattering chamber has a

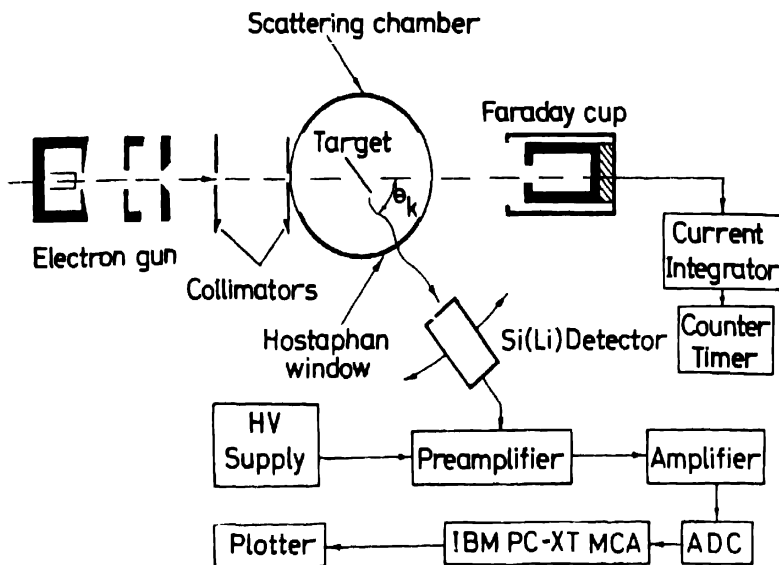


Fig. 1. Schematic diagram of a complete experimental setup for measuring the bremsstrahlung spectra from a target of pure elements.

movable target holder with a facility of positioning the multiple targets one at a time without cycling the vacuum of the system.

A Faraday cup is mounted on the other collinear port through a KF10 coupling. The cup has two coaxial hollow Al cylinders; the inner cylinder collects the charge which has transmitted through the target while the outer cylinder is used to bias the cup for preventing the secondary electrons from escaping the inner cylinder [see, Fig. 1]. In case of thick targets, the current monitoring is, however, done on the target itself (as, in the present experiments).

Thin foils of the solid targets of pure elements are mounted on an aluminum frame having four consecutive holes, each 12.0 mm in diameter. The frame is attached on an insulated SS shaft which enables one to position the foils at a desired place and at a chosen orientation with respect to the incident electron beam direction.

A Canberra Si(Li) x-ray photon detector (FWHM = 250 eV at 5.9 keV) is placed on an Al platform (530 mm x 250 mm x 10 mm) which can rotate about the collision centre. The detector sits outside the main scattering chamber at about 57 mm from the collision centre and detects photons through its 25- $\mu$ m Be window. The detector can be rotated about the interaction zone

between  $30^\circ$  and  $150^\circ$  on one side and  $210^\circ$  and  $270^\circ$  on the other side of the collinear ports with a precision of  $\pm 1^\circ$ .

### **3.2 High-voltage electron gun**

We have taken the electron gun (EG) out from a discarded CRO and have modified its indirectly heated, oxide coated cathode by an assembly with a replaceable  $\Lambda$ -shaped hair-pin tungsten filament. A pair of voltage/current feed-throughs are incorporated in the assembly. This modified arrangement with a 'replaceable filament' is desirable because it allows us to operate the gun with frequent exposures to atmosphere. The tungsten filament is more rugged and resistant to oxidation. The filament is found to have an average lifetime of about 100 hours when operated at 2.2 V/3A. The other components of the EG are control grid, anode, focusing electrode, X- and Y- deflection plates and the input and output terminals. The complete EG is made to rest vertically on a perspex flange with three Al pillars attached to the base of the gun. An aluminum enclosure of a suitable dimensions houses the EG and is mounted horizontally on the main scattering chamber through a KF10 coupling. Further, a slit assembly of carbon apertures ( $\varnothing \sim 3.0$  mm) is fitted between the main scattering chamber and the EG enclosure which facilitates in rendering a well collimated electron beam on the target.

### **3.3 Isolated, floating high-voltage unit**

In order to keep the anode at earth potential and the cathode/grid at a high negative voltage, it was essential to develop an isolated, floating high-voltage system. For this purpose, an 20 kV isolation transformer was used to keep the main line isolated from high voltages (d.c.). Necessary grounding for high voltages and for other units was derived from a common earthing point. All units floating on a high negative voltage are enclosed in an insulated metallic cage which is properly earthed. The regulation of the filament power supply and that of the grid power supply enclosed in the cage was achieved by the perspex shafts attached to the knobs of the power supplies. The two highly regulated high-voltage d.c. power supplies (0-20 kV, 0-1.5 mA) were used to provide the accelerating and the focusing voltages to the respective electrodes. The uncertainty in the input voltage to the electrode is not more than 1%. A typical set of values for voltage/current applied on various electrodes of the EG for obtaining a well collimated electron beam of 6.0 nA on a thin Ag foil is presented in Table 1.

A visual check of the dimensions of the beam spot ( $\varnothing \sim 3.0$  mm) on the target was made on a ZnS screen placed on the target's position. Further, it

Table 1. Characteristic values for various voltages and current applied to electron gun electrodes for a 6.0 nA beam on a Ag target at 6.0 kV accelerating potential.

Filament voltage / current	2.1 V / 3.0 A
Cathode voltage / emission current	-6.0 kV / 0.007 mA
Focusing voltage / emission current	-5.92 kV / 0.0 mA
Grid voltage	-0.5 V
X <sub>1</sub> / X <sub>2</sub> deflector plates	100 V / 0 V
Y <sub>1</sub> / Y <sub>2</sub> deflector plates	100 V / 0 V
Beam spot size	Ø ~ 0.3 cm

was found that the positioning of the filament tip with respect to the grid-hole is very critical for obtaining a properly focused electron beam at the target position [6].

### 3.4 High-vacuum pumping system

The electron-gun enclosure was evacuated by a 4.5~ oil diffusion pump (300 l/s) while the main scattering chamber was evacuated by a 2.5~ oil-diffusion pump (100 l/sec). The pressures maintained by rotary and diffusion pumps were measured by the Pirani and the Penning gauges respectively. The base pressure attained in the scattering chamber and that in the electron gun enclosure were usually better than  $2 \times 10^{-6}$  mbar without using a liquid nitrogen trap. Both pumping units were purchased from M/S Hind High Vacuum Company Ltd., Bangalore, India.

### 3.5 Signal processing and data acquisition system

A block diagram for the data production and their handling system is shown in Fig. 2. The photon signals generated by the Si(Li) detector is amplified, shaped and digitized by the standard NIM electronic modules and are finally accumulated by an IBM PC/XT based 4K multichannel analyzer (MCA) in a pulse-height analysis (PHA) mode. The data acquisition, stripping, plotting, etc., are carried out on this computer. The beam collected on the insulated targets in the present experiments was monitored by a pico-ammeter and integrated by a digital current integrator.

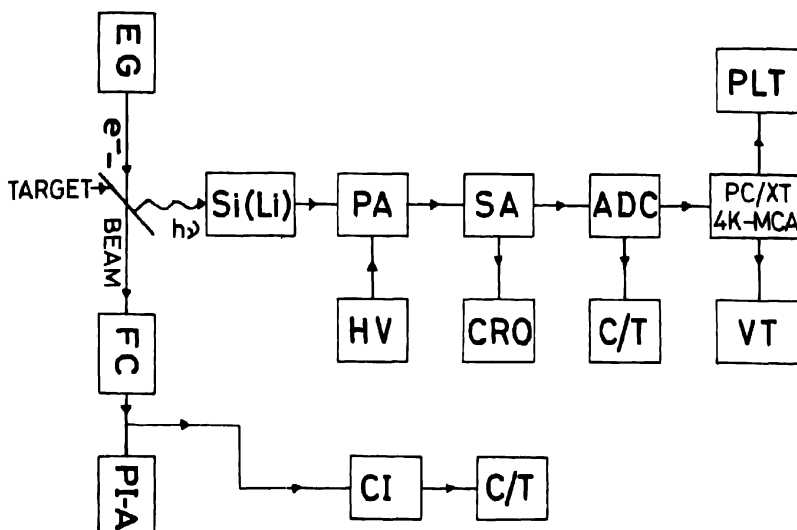


Fig. 2. Block diagram of the signal processing and the data acquisition system. PA: Preamplifier; SA: spectroscopy Amplifier; ADC: Analogue to digital converter; HV: high-voltage power supply; PLT: Plotter; CRO: Cathode ray oscilloscope; C/T: Counter timer; VT: Video terminal; CI: Current Integrator; PI-A: Pico-ammeter; FC: Faraday cup; EG: Electron gun.

#### 4. Experimental procedure and bremsstrahlung energy spectra

The experiments were carried out after ensuring that the base pressure of the system is maintained at about  $2 \times 10^{-6}$  mbar, and there is a stable electron beam falling on the sample. The detector was optimized for the best signal-to-noise ratio by using a standard  $^{55}\text{Fe}$  radioactive source placed at the target position. Accumulation of a desired AFB spectrum for a given target and electron-energy combination was made at a photon emission angle of  $\theta_k = 90^\circ$ . Since the AFB intensity depends on  $Z^2$  ( $Z$  = atomic number of the target) and on the beam current, the data collection times of 20-30 minutes with a beam current of 1-3 nA on the targets having  $Z = 40-80$  was found to be more than sufficient for a channel-to-channel counting statistics of less than 10%.

In AFB spectra, the background radiation is a most serious problem to account for. This radiation arises due to the elastic and the inelastic events of scattering of the incident electrons from the materials in the vicinity of the targets used. In particular, the thick-target bremsstrahlung radiation originated in the region being away from the beam-target interaction zone and eventually seen by the detector in a given geometrical configuration contributes maxi-

mum. This problem can be circumvented to a large degree by collimating the incident beam with a set of narrow slits and by limiting the solid angle of the photon detector with respect to the target. The latter can be readily accomplished by using a narrow aperture on the detector's window. The background radiation is a function of impact energy of the electrons and of the nature of thick materials around the interaction zone. In order to reduce the intensity of the background radiation, it is always preferred to use a low-Z material for constructing the target frame. Generally, the background radiation is recorded by introducing the empty frame in front of the beam. Nevertheless, this method is good enough as long as there is a small probability of the incident electrons being - elastically scattered from the target and producing radiation in the thick walls of the chamber and in the window. In AFB spectra, the background subtraction has to be done with great care.

We have recorded the bremsstrahlung energy spectra from thin foils of Ag ( $150 \mu\text{g}/\text{cm}^2$ ), and Au ( $200 \mu\text{g}/\text{cm}^2$ ) bombarded by 7.0-keV electrons. The photon detector was placed at  $90^\circ$  and the foils were tilted at  $45^\circ$  to the incident electron beam direction. The pulse height spectra of the bremsstrahlung radiation was recorded in a 4K MCA whose channels were energy calibrated by using a standard  $^{55}\text{Fe}$  radioactive source. It should be mentioned here that the above targets are thick enough to arrest all the electrons that impinge on the target, but they are thin enough to transmit a large fraction of photons produced in the interaction zone. Thus, no current monitoring was done on the Faraday cup. Instead, the current is monitored on the insulated target itself.

## 5. Relative shape of the bremsstrahlung energy spectrum

The relative shape of the bremsstrahlung photon-energy spectrum from 7.0 keV electrons incident on Ag and Au was determined from the obtained spectra as described in Section 4. Since the theory [7] is believed to be accurate in the shape of the photon energy dependence to about 5% or better, it is desirable to have experimental data of this precision. For this, we have considered the ratio of the doubly differential cross sections ( $\text{DDCS} \equiv d^2\sigma/dk d\Omega$ ) for Ag and Au targets at the same incident energy and photon emission angle, it was possible for us to obtain the relative shape of the photon-energy spectrum to a precision of better than 4%.

The number of bremsstrahlung photons of energy  $k$  [ $N_B(k)$ ] detected by a Si(Li) detector with a solid angle  $\Delta\Omega$  within an energy width of  $\Delta k$  is given by,



$$N_B(k) = N_0 N_t \left[ \frac{d^2\sigma}{dkd\Omega} \right] \Delta k \Delta\Omega \epsilon(k) \quad (1)$$

where,  $N_0$  is the total number of electrons incident on the target,  $N_t$  is the number of target atoms per  $\text{cm}^2$ , and  $\epsilon(k)$  is the detector efficiency at  $k$ .

The ratio of the theoretical bremsstrahlung DDCS for Ag and Au with their respective atomic numbers  $Z_{\text{Ag}}$  and  $Z_{\text{Au}}$  for the same values of  $T$ ,  $k$  and  $\theta_k$  when compared with the experimental DDCS can be expressed by a relation,

$$\left[ \frac{d^2\sigma^{\text{Ag}}}{dkd\Omega} / \frac{d^2\sigma^{\text{Au}}}{dkd\Omega} \right]_{\text{theory}} / \left[ \frac{d^2\sigma^{\text{Ag}}}{dkd\Omega} / \frac{d^2\sigma^{\text{Au}}}{dkd\Omega} \right]_{\text{exp}} = R \frac{N_B^{\text{Ag}}(k)}{N_B^{\text{Au}}(k)} \quad (2)$$

where,  $R = (N_0 N_t)_{\text{Au}} / (N_0 N_t)_{\text{Ag}}$ . While taking the ratio of DDCS, the solid angle  $\Delta\Omega$ , the detector efficiency  $\epsilon(k)$  and the chosen energy width  $\Delta k$  are cancelled out. Thus, the ratio depends only on the target thickness and on the total number of incident electrons. The individual uncertainties in these quantities have no effect on the photon energy dependence of the cross section ratios. The total uncertainty is thus reduced to a much smaller value that stems from the uncertainties in the incident electron energy and in counting statistics. This has amounted in the present case to less than 4% which is comparable to the theoretical uncertainty of 5%.

Fig. 3 shows the bremsstrahlung data for the DDCS ratios for Ag and Au targets with 7.0-keV electron impact as a function of the fraction of photon energy radiated ( $k/T$ ). The experimental data are found to overestimate the theory by about 20%. The relative shape of the photon-energy spectrum however, remains unchanged at all photon energies between  $k = 4.0$ -7.0 keV as per theoretical predictions. The above discrepancy is suggested to be due to arise from the thick-target effects; for further details of the analysis and results, see Ref. [8].

Figs. 4 and 5 show the thick-target bremsstrahlung energy distributions as a function of photon energy  $k$  for 7.0-keV electrons on Ag ( $150 \mu\text{g}/\text{cm}^2$ ) and ( $200 \mu\text{g}/\text{cm}^2$ ). The data have been compared [9,10] with two models: (i) a modified Kramers-Kulenkampff-Dyson formula (KKD model), and (ii) a semiempirical expression after the spectra were corrected for electron back-scattering, energy loss, photon attenuation in the target and for inherent filtration. The KKD model is found to give good agreement with experiment, although it predicts a shift in maximum intensity towards the high photon-energy side for Au while it agrees well for Ag. On the other hand, the semi-

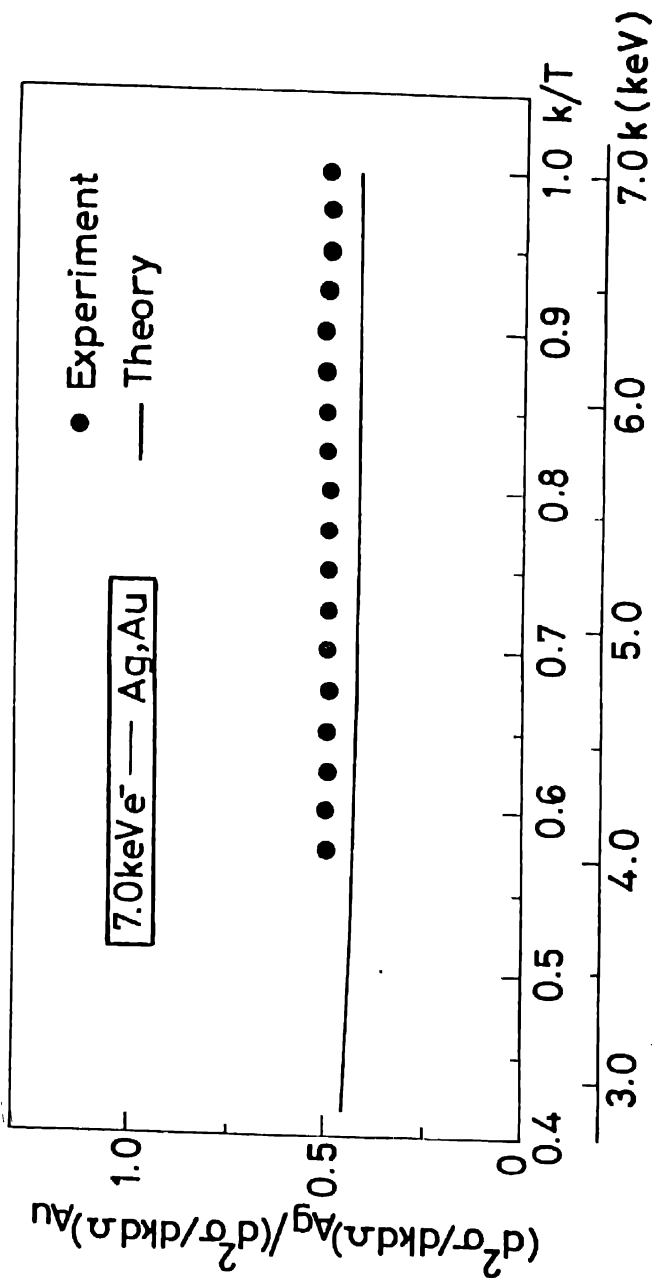


Fig. 3. Ratio of the DDCS of bremsstrahlung photons for 7.0-keV electrons incident on Ag (150  $\mu\text{g}/\text{cm}^2$ ) and Au (200  $\mu\text{g}/\text{cm}^2$ ) plotted as a function of photon energy radiated ( $k/T$ ). ● present data; — theory (Ref. 7).

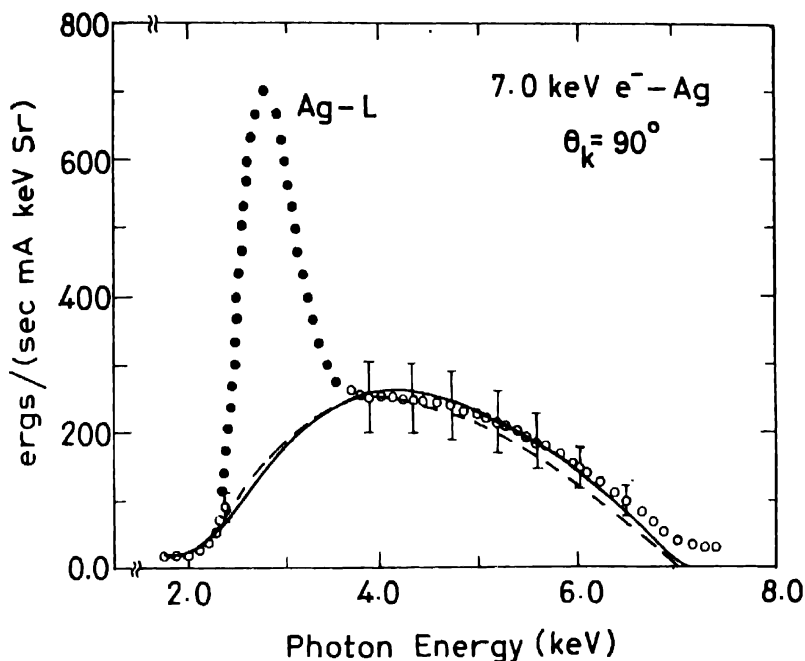


Fig. 4. Thick-target bremsstrahlung energy-distribution as a function of photon energy for 7.0-keV electrons on Ag. (○) : present data; --- : modified KKD formula; - · - : semiempirical formula. Error bars refer to the experimental systematic error.

classical formula which is an approximation to the Born-approximation thin-target formula with electron-energy and bremsstrahlung losses multiplied by a photon-attenuation correction gives a better fit to the data for both targets. Although both models are found to give overall agreement with the data to within the systematic error of 21% on absolute scale, it is felt necessary that the depth distribution of the electrons as a function of their residual energies must be taken into account. Thus, the connection between the thick-target spectra and the thin-target bremsstrahlung prediction requires a comprehensive theory of the passage of electrons through matter.

## 6. Summary

A brief description of a dedicated, indigenous experimental setup for studying the atomic-field-bremsstrahlung process with keV electrons interacting with a solid, pure elemental target is presented. The design and fabri-

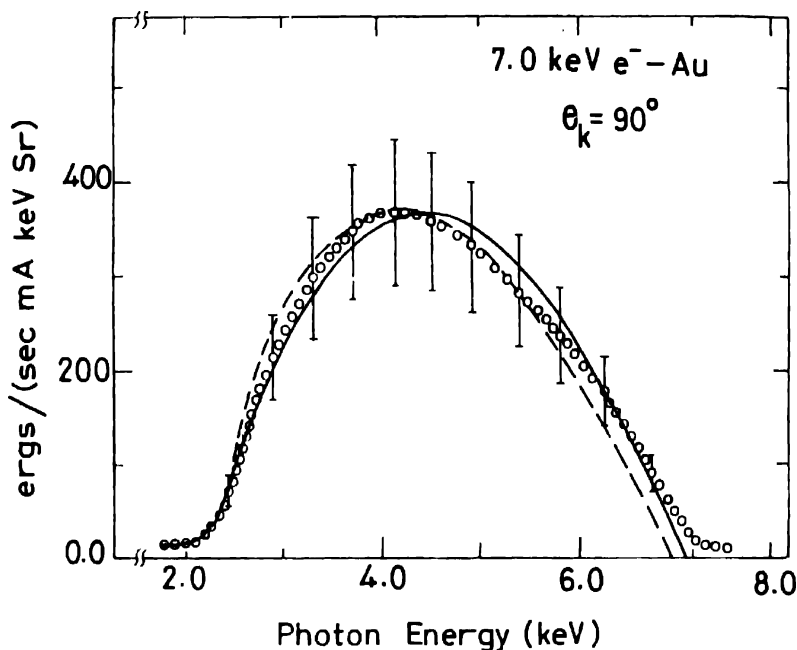


Fig. 5. Same as for Fig. 4 except for the Au-target.

cation of various components involved in the setup has been described. The facility has been tested, optimized for a well collimated electron beam of about 3 mm spot size on the target. The electron gun has been operated up to 8.0-kV accelerating potential. A few typical bremsstrahlung energy spectra from Ag and Au targets have been presented and discussed. A comparison of the data with the available thin- and thick-target theories have been made. The agreement between experiment and theory is found to be satisfactory within the uncertainty of the measurements.

It may be mentioned here that the estimated cost of the above system is about 5-6 times lesser than a custom-built unit.

### Acknowledgments

I am thankful to my student M. J. Singh for their contributions in designing, fabricating and operating the above facility. The financial support from the Department of Science and Technology, New Delhi is gratefully acknowledged.

## References

- [1] R. H. Pratt, *Comm. Atom Mol. Phys.* **10**, 139 (1981)
- [2] W. Nakel, in *Innershell and X-ray Physics of Atoms and Solids*, edited by D. Fabian, H. Kleinpoppen and L. M. Watson (Plenum Press, N.Y., 1981).
- [3] R. Ambrose, D. L. Kahler, H. E. Lehtihet and C. A. Quarles, *Nucl. Instr. Methods B* **56/57**, 327 (1991); C. A. Quarles and D. B. Heroy, *Phys. Rev. A* **24**, 48 (1981), and references therein.
- [4] R. Hippler, K. Saeed, I. McGregor and H. Kleinpoppen, *Phys. Rev. Lett.* **48**, 1622 (1981).
- [5] S. K. Goel, M. J. Singh and R. Shanker, *Pramana* **45**, 2911 (1995).
- [6] O. Klemperer, *Electron Optics*, Cambridge Monographs on Physics (Cambridge at University Press, 1971) pp. 320-388.
- [7] L. Kissel, C. A. Quarles and R. H. Pratt, *At. Data Nucl. Data Tables* **28**, 381 (1983).
- [8] S. K. Goel, M. J. Singh and R. Shanker, *Phys. Rev. A* **52**, 2453 (1995).
- [9] S. K. Goel and R. Shanker, *Phys. Rev. A* (1996) in press.
- [10] S. K. Goel, Ph.D. dissertation, Banaras Hindu University, Varanasi, 1996.